Combination of a Rapamycin Analog (CCI-779) and Interferon-γ is More Effective than Single Agents in Treating a Mouse Model of Tuberous Sclerosis Complex

Laifong Lee, Paul Sudentas, and Sandra L. Dabora*

Hematology Division, Department of Medicine, Brigham and Women's Hospital, Karp Family Research Laboratories, Boston, MA 02115

Tuberous sclerosis complex (TSC) is a familial tumor syndrome characterized by the development of hamartomas in the brain, heart, kidney, and skin. Disease-causing mutations in the *TSC1* or *TSC2* gene result in constitutive activation of the highly conserved mTOR signal transduction pathway, which regulates cell growth, proliferation, and metabolism. The mTOR inhibitor, rapamycin (sirolimus), reduces disease severity in rodent models of TSC, and is currently in phase II clinical trials. The cytokine interferon-gamma (IFN-γ) is another potential therapeutic agent for TSC. A high-expressing IFN-γ allele is associated with a lower frequency of kidney tumors in TSC patients, and treatment with exogenous IFN-γ reduces the severity of TSC-related disease in mouse models. Here, we examine the effects of treating tumor-bearing nude mice with a combination of a rapamycin analog (CCI-779) and IFN-γ. We observed that combination therapy was more effective than single agent therapy in reducing tumor growth and improving survival in this mouse model of TSC. Immunoblot and immunohistochemical analyses showed that tumors treated with CCI-779 plus IFN-γ had decreased cell proliferation and increased cell death in comparison with untreated tumors or tumors treated with either agent alone. We also observed that CCI-779 resistance could develop with prolonged treatment. Taken together, our results show that targeting multiple cellular pathways is an effective strategy for treating TSC-related tumors, and underscore the importance of investigating combination therapy in future clinical trials for patients with TSC.

INTRODUCTION

Tuberous sclerosis complex (TSC) is a multisystem familial tumor syndrome characterized by the development of hamartomas in the brain, skin, kidney, and heart (Kwiatkowski and Short, 1994; Gomez, 1995; Cheadle et al., 2000; Online Mendelian Inheritance in Man, 2003b). TSC patients face various medical problems, including epilepsy, cognitive impairment, behavioral issues, brain lesions (tubers and/or subependymal nodules), skin tumors (facial angiofibromas), cardiac tumors (rhabdomyomas), kidney cysts, kidney tumors (angiomyolipomas), and pulmonary abnormalities including lymphangiomyoleiomatosis (LAM) (Gomez, 1995; Dabora et al., 2001; Franz et al., 2001; Online Mendelian Inheritance in Man, 2003a).

TSC is caused by the loss of function of either of two genes, *TSC1* or *TSC2* (Cheadle et al., 2000). The products of these genes, tuberin and hamartin, function in the highly conserved mTOR signal transduction pathway, which regulates cell growth, proliferation, and metabolism (Potter et al., 2001; Gao et al., 2002). The tuberin/hamartin complex is a negative regulator of the mTOR kinase. In cells lacking tuberin and/or hamartin, constitutive activation of mTOR results in hyperphosphorylation of its downstream substrates, p70 S6 kinase (S6K) and eukaryotic initiation factor 4E binding protein 1 (4EBP1) (Findlay et al., 2005; Inoki et al., 2005). Since cells lacking tuberin or hamartin lack inhibition of mTOR, one obvious strategy for treating TSC is to restore that inhibition.

Rapamycin (sirolimus) is a macrolide antibiotic that can inhibit mTOR and is currently used as an immunosuppressive drug to prevent renal graft rejection (Hidalgo and Rowinsky, 2000; Garber,

Supported by: Tuberous Sclerosis Alliance, NIH (NIDDK); Grant number: DK066366, NIH (NCI); Grant number: P50CA101942.

*Correspondence to: Sandra L. Dabora, Hematology Division, Brigham and Women's Hospital, Karp Family Research Laboratories, 6th Floor, 1 Blackfan Circle, Boston, MA 02115, USA.
E-mail: sdabora@partners.org

Received 24 January 2006; Accepted 5 June 2006

DOI 10.1002/gcc.20357

Published online 14 July 2006 in Wiley InterScience (www.interscience.wiley.com).

2001). The potential benefit of rapamycin or rapamycin analogs in TSC rodent models has been shown (Hino et al., 2002; Kenerson et al., 2002; Kenerson et al., 2005; Lee et al., 2005). Rapamycin clinical trials are now ongoing to assess the safety of the drug in patients with TSC and LAM, and to investigate the effect of rapamycin on the size of renal angiomyolipomas in these patients (Bissler et al., 2004; Wienecke et al., 2004; http://clinicaltrials.gov/show/NCT00126672). CCI-779 (temsirolimus) is an ester derivative of rapamycin, developed by Wyeth-Ayerst Pharmaceuticals, that is more suitable for i.v. formulation. The antitumor effect of CCI-779 has been demonstrated in a variety of tumor types (Mills et al., 2001; Neshat et al., 2001; Podsypanina et al., 2001; Yu et al., 2001; Frost et al., 2004), and CCI-779 is currently in phase III trials for development as an anticancer agent (Vignot et al., 2005).

Another potential therapeutic agent for the treatment of TSC disease is the cytokine interferon-gamma (IFN-γ). A marked reduction in the frequency of kidney tumors has been reported in $Tsc2^{+/-}$ mice with elevated endogenous IFN-γ compared to that in $Tsc2^{+/-}$ mice with normal (low) IFN-γ levels (Hino et al., 2002). We have observed a decreased frequency of kidney angiomyolipomas in the presence of a high-expressing IFN-γ allele in a cohort of TSC patients (Dabora et al., 2002). More recently, we have demonstrated that treatment with exogenous IFN-γ decreases disease severity in mouse models of TSC (Lee et al., 2005).

IFN-γ-regulated genes have a vast array of functions, including antigen processing and presentation, immunomodulation, inhibition of cell proliferation, and induction of apoptosis (Schroder et al., 2004). IFN-γ primarily signals through the JAK-STAT signal transduction pathway, in which its binding to the IFN-γ receptor results in a cascade of events including phosphorylation and activation of the Jak1, Jak2, and Stat1 proteins (Schroder et al., 2004). Stat1 plays a key role in controlling the transcription of IFN-γ-regulated genes, as indicated by the phenotype of $Stat1^{-/-}$ mice, which largely phenocopy mice lacking one of the IFN-γ receptor chains (Meraz et al., 1996). There is also emerging evidence that Stat1 is involved in inhibiting cell growth and promoting apoptosis (Bromberg, 2001).

In a previous study, we demonstrated that CCI-779 and IFN-γ, used as single agents, were effective in decreasing disease severity in mouse models of TSC (Lee et al., 2005). We now report that combination therapy with CCI-779 and IFN-γ is more effective than treatment with either agent alone in reducing tumor growth and improving survival in a nude mouse model of TSC. Tumors treated simultaneously with both agents show increased apoptosis and decreased cell proliferation in comparison with untreated tumors or tumors treated with either agent alone.

MATERIALS AND METHODS

Induction of s.c. Tumors in Nude Mice

Nude mice (strain CD-1nuBR, 8–9 weeks old) were obtained from Charles River Laboratories (Wilmington, Massachusetts). For the long-term treatment trial, 40 nude mice were injected s.c. on the dorsal flank with 2.5 million NTC/T2null ($Tsc2^{-/-}$, $Trp53^{-/-}$) cells. Tumors were measured with calipers three times a week. Tumor volumes were calculated by use of the formula $L \times W \times W \times 0.5$ (Torrance et al., 2001). When tumor volumes were $\geq$300 mm^3, mice were randomly assigned to four cohorts: untreated, CCI-779-treated, IFN-γ-treated, and CCI-779 plus IFN-γ-treated (referred to hereafter as combination-treated). Mice were euthanized when tumor volumes exceeded 2,500 mm^3, and within 2–4 hr after the final treatment. One mouse was euthanized before its tumor volume reached 2,500 mm^3 because of the presence of a nonhealing ulcer. For the short-term treatment trial, 24 nude mice were injected s.c. on the dorsal flank with 2.5 million NTC/T2null cells. When tumor volumes were $\geq$200 mm^3, mice were randomly assigned to the same four cohorts listed previously. Mice were assigned at a lower tumor volume than that of the long-term trial because we had previously observed significant necrosis in untreated tumors that were $\geq$300 mm^3, which complicated the analysis of apoptosis in treated tumors. Tumor volumes were measured every day. Untreated mice were euthanized when tumor volumes were 260–320 mm^3. Treated mice were euthanized after 2–5 treatments within 2–4 hr after the final treatment. All tumor-bearing animals were euthanized according to institutional animal care guidelines, based on tumor size or presence of an open ulcer. Tumor tissue was harvested for histopathologic analysis, and tumor lysates were prepared for immunoblot analysis.

Treatment of Mice with CCI-779 and IFN-γ

Tumor-bearing nude mice in the long-term treatment trial were treated 5 days a week (Monday–Friday) by i.p. injection (IP). CCI-779 was administered at a dose of 8 mg/kg. A 30 mg/ml stock solution of CCI-779 was made in ethanol (stored at

20°C for up to 1 week), diluted to 0.6 mg/ml in vehicle (0.25% PEG, 0.25% Tween-20), and used within 24 hr. Murine IFN-γ was administered at a dose of 20,000 units (2.4 μg). Murine IFN-γ was diluted to 1 × 100,000 units/ml in PBS containing 0.1% mouse serum albumin (Sigma-Aldrich, Saint Louis, Missouri) and stored at 4°C for up to 1 week. Tumor volumes were measured 3 days a week; therefore, every 3 days of measurement corresponded to ~1 week. One animal died of unknown causes before being assigned to a cohort and before development of a measurable tumor. The average time to assignment (day of injection to the day when tumor volume was $\geq$300 mm^3) was 47 days. Only animals with time to assignment within two SDs of the average were included in the final analysis. Based on this criterion, two animals were excluded from the final analysis (one from the CCI-779-treated cohort, and one from the combination-treated cohort). Therefore, there were a total of 37 mice in the final analysis: 9 each in the CCI-779-, IFN-γ-, and combination-treated cohorts, and 10 in the untreated cohort. We did not observe any significant toxicity from the treatments; mice were weighed before and after treatment, and no significant changes were observed.

Tumor-bearing nude mice in the short-term treatment trial were treated on consecutive days by IP with the same CCI-779 and IFN-γ dosage as that of the long-term trial. Our goal was to collect tumors that were $\leq$350 mm^3, and so, the number of treatments ranged from 2–5. The average number of treatments in the CCI-779-treated, IFN-γ-treated, and combination-treated cohorts were 3.7, 2.7, and 4.5, respectively. All experiments were done according to animal protocols approved by our institutional animal protocol review committee and were compliant with federal, local, and institutional guidelines on the care of experimental animals.

Immunoblot Analysis

Immunoblot analyses of tumor tissue and cultured cell lysates were performed as described previously (Kwiatkowski et al., 2002), and protein was detected by chemiluminescence (Pierce, Rockford, IL). Anti-pStat1 (Ser727), anti-IRF-1, anti-MPP2 (FoxM1), anti-PCNA, anti-FAS, anti-goat IgG-HRP, anti-rabbit IgG-HRP, and anti-mouse IgG-HRP antibodies were purchased from Santa Cruz Biotechnology (Santa Cruz, CA). Anti-pS6 (Ser235/236), anti-Stat1, anti-pStat1 (Tyr701), anti-cyclin D1, anti-caspase-3, anti-caspase-9, and anti-caspase-12 antibodies were purchased from Cell Signaling Technology (Beverly, MA). Anti-S6 antibody was synthesized by Sigma Genosys (The Woodlands, TX). Anti-actin antibody was purchased from Sigma–Aldrich (Saint Louis, MO).

We observed some variability from tumor to tumor within a cohort with regard to treatment-induced changes in the levels of the proteins examined. Therefore, all tumors from all cohorts were analyzed, and the intensity of bands from the immunoblot analyses was quantified by densitometry. Densitometry measurements were performed using Adobe Photoshop Elements 2.0 software. Intensity of each band was standardized to a loading control (actin), and results from all samples in a cohort were averaged and compared with the average from the untreated cohort.

Analysis of Apoptosis

At necropsy, the largest cross section of each tumor was fixed for paraffin embedding, sectioning, and staining with H&E. Unstained slides were also made (HSRL, Mt. Jackson, VA). Apoptotic cells in the tumors were detected by the TUNEL assay, using the ApopTag Plus Peroxidase In Situ Apoptosis Detection Kit from Chemicon International (Temecula, CA). To quantify the percentage of apoptotic cells in each tumor, slides were coded and 5–10 digital images were obtained from nonnecrotic areas of each tumor. The number of cells that stained positive (dark brown) for apoptosis as well as the total number of cells were counted. Microscopy was done with a Nikon Eclipse TE 2000-E microscope (Nikon Corporation, Tokyo, Japan) using a 20× objective equipped with an Insight SPOT color camera (Micro Video Instruments, Avon, MA).

Cell Lines and *In Vitro* Studies

The NTC/T2null cell line is a $Tsc2^{-/-}$, $Trp53^{-/-}$ mouse embryonic fibroblast cell line that has been previously described (Lee et al., 2005). All cells were grown in Dulbecco's Modified Eagle Medium (DMEM) with 10% FCS in 5% CO_2. DMEM and FCS were purchased from Fisher Scientific (Pittsburgh, PA). CCI-779 was added to cell cultures at a concentration of 20 nM, and murine IFN-γ was added at a concentration of 10 ng/ml. Cells were collected at 3, 24, 48, and 72 hr after addition of treatment agent(s) for lysate preparation and immunoblot analysis. CCI-779 was obtained from Wyeth-Ayerst Pharmaceuticals (Madison, NJ). Murine IFN-γ was purchased from R&D Systems (Minneapolis, MN).

Statistical Analysis

GraphPad Prism (version 4) software was used for all statistical analyses, and $P < 0.05$ was considered to indicate significance. The Fisher test was used for categorical variables; the *t* test was used for quantitative variables; and Mantel-Cox logrank analysis was used for survival data.

RESULTS

CCI-779 Plus IFN-γ Combination Treatment is More Effective than CCI-779 in Reducing Tumor Growth and Improving Survival in a Nude Mouse Model of TSC

To determine whether the combination of CCI-779 and IFN-γ is more effective than using the drugs as single agents in a preclinical model for TSC-related tumors, we evaluated tumor growth and survival in cohorts of nude mice bearing $Tsc2^{-/-}$ tumors. Nude mice were given s.c. injections of NTC/T2null cells (referred to hereafter as $Tsc2^{-/-}$ cells) in the dorsal flank to induce development of TSC-related tumors. When tumor volume was ≥300 mm^3, mice were randomly assigned to four cohorts: untreated, IFN-γ-treated, CCI-779-treated, and combination-treated. Tumor volumes were measured three times a week, and mice were euthanized when tumor volumes exceeded 2,500 mm^3 (see Materials and Methods). The study design here differs from our prior study (Lee et al., 2005) because tumors were significantly larger when treatment was initiated in this study.

Consistent with our previous observations (Lee et al., 2005), treatment with CCI-779 or IFN-γ as single agents reduced tumor growth (Fig. 1). At week 2 (day 6 of measurement), the average tumor volumes of the IFN-γ-treated group (2,183 ± 201 mm^3) and the CCI-779-treated group (387 ± 33 mm^3) were lower than that of the untreated group (3,074 ± 341 mm^3) (Table 1). In this experiment, improved survival was observed with CCI-779, but not with IFN-γ treatment. Because CCI-779 appears to be more effective than IFN-γ, it is more relevant to compare the antitumor effect of combined CCI-779 plus IFN-γ with that of CCI-779.

As shown in Figure 1a, TSC-related tumors from the combination-treated nude mice grew at a slower rate than tumors from CCI-779-treated mice. At week 6 (day 16 of measurement), when the first mouse from the CCI-779-treated cohort was euthanized, the average tumor volume from the combination-treated group was 1.8-fold less than the average tumor volume from the CCI-779-treated group (1,610 ± 269 mm^3 versus 3,000 ± 378 mm^3; $P = 0.0085$ (*t* test); see Table 1). In fact, the majority of tumors regressed during the first 2 weeks (7/9 in the CCI-779-treated cohort and 6/9 in the combination-treated cohort), resulting in average tumor volume decreases of 14.0 ± 4.4 and 2.9 ± 5.5 mm^3/day in the CCI-779- and combination-treated cohorts, respectively. Beyond 2 weeks of treatment, the tumors resumed progressive growth, but the combination-treated cohort grew at a slower rate (50.6 ± 7.8 mm^3/day) than the CCI-779-treated cohort (110.2 ± 15.7 mm^3/day).

Interestingly, at week 2, there was no significant difference in average tumor volumes between the CCI-779-treated cohort and the combination-treated cohort (387 ± 33 mm^3 versus 432 ± 89 mm^3) (Table 1).

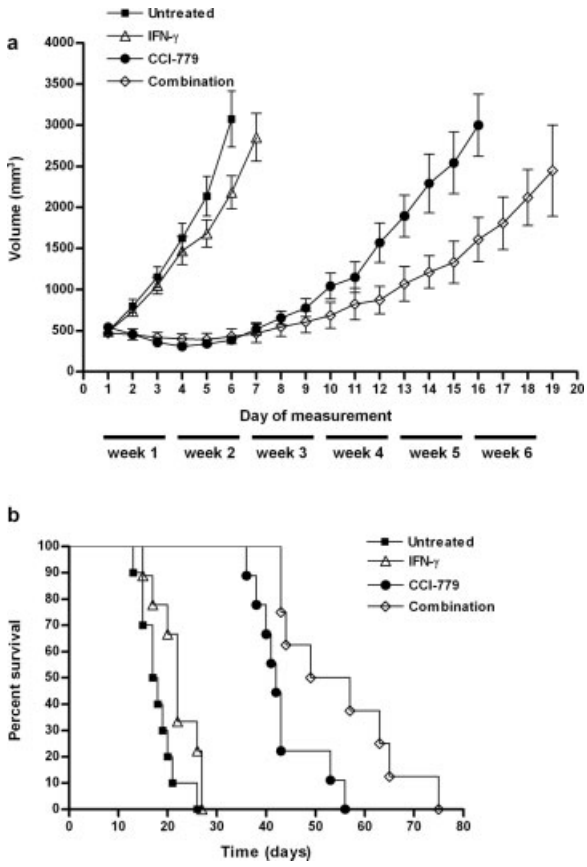

Figure 1. Improved survival and decreased tumor growth with CCI-779 plus IFN-γ combination treatment. (a) Average tumor growth over time for indicated treatment cohorts. On day 6 of tumor measurement (week 2, the day that the first untreated mouse was euthanized), the average tumor volumes were lower in the IFN-γ- ($P = 0.04$) and CCI-779- ($P < 0.0001$) treated cohorts versus the untreated cohort. On day 16 of treatment (week 6, the day the first CCI-779-treated mouse was euthanized), the average tumor volume was lower in the combination-treated cohort versus the CCI-779-treated cohort ($P = 0.0085$). (b) Survival curve for indicated treatment cohorts. Mantel-Cox logrank analysis shows improved survival in the cohort treated with CCI-779 plus IFN-γ versus the cohort treated with CCI-779 as a single agent ($P = 0.0028$).

TABLE 1. Analysis of Survival and Tumor Growth in Long-term Treatment Trial

	Untreated	IFN-γ-treated	CCI-779-treated	Combination-treated
Median survival (days)	17.5	22.0	41.0	56.0
P value			<0.0001*	0.0028**
Average tumor volume (mm^3)				
At assignment	495 ± 45	491 ± 42	542 ± 58	472 ± 58
Week 2	3074 ± 341	2183 ± 201	387 ± 33	432 ± 89
P value		0.04*	<0.0001*	<0.0001*
Week 6	NA	NA	3000 ± 378	1610 ± 269
P value				0.0085**
N (mice)	10	9	9	9

*When compared with untreated.
**When compared with CCI-779-treated.

The increased efficacy of combination treatment versus CCI-779 treatment becomes apparent only during weeks 3–4 of treatment. Some differences in the clinical response of the tumors to the treatment agent(s) were observed within each cohort, possibly because of the heterogeneity of the $Tsc2^{-/-}$ tumors. The ranges of average tumor growth per day (from day of assignment to day when the first mouse in the cohort was euthanized) were: 169.6–442.0, 53.3–114.7, 155.9–306.9, and 17.8–127.3 mm^3 for the untreated, CCI-779-treated, IFN-γ-treated, and combination-treated cohorts, respectively.

CCI-779 plus IFN-γ combination treatment resulted in improved survival in comparison with CCI-779 treatment (Fig. 1b). The median survival of the combination-treated cohort was 56 days versus a median survival of 41 days in the CCI-779-treated cohort (Mantel-Cox logrank analysis; $P = 0.0028$, see Table 1). Treatment with CCI-779 as a single agent also improved survival (versus no treatment), but less effectively than treatment with combined CCI-779 plus IFN-γ. We did not observe improved survival with single agent IFN-γ treatment in this trial. This differs from the results in our previous report (Lee et al., 2005) and is likely due to the later initiation of treatment when tumors were $\geq$300 mm^3. This difference suggests that IFN-γ is more effective in treating early tumors.

Since the experiment described earlier was designed to determine the effects of treatment(s) on overall tumor growth and survival, the TSC-related tumors in all cohorts were grown to a volume of over 2,500 mm^3 before the mice were euthanized. In the CCI-779- and combination-treated cohorts, tumor growth was minimal during the first 2 weeks of treatment, and in the majority of animals, tumor regression was observed. However, after 2 weeks of treatment, all tumors resumed progressive growth, possibly because of the development of resistance to treatment agent(s). To analyze tumors that were still showing marked response to treatment, a short-term treatment trial was carried out. The cohorts in this short-term trial were identical to those in the long-term trial (untreated, IFN-γ-treated, CCI-779-treated, and combination-treated), but treated animals received only 2–5 treatments on consecutive days, and tumor volume was measured every day. The number of treatments ranged from 2–5 because we wanted to collect tumors that were $\leq$350 mm^3 to minimize the necrosis that occurs, regardless of treatment, with increasing tumor size.

The effect of short-term treatments on tumor growth was analyzed by comparing the average tumor volume change per day in the untreated versus treated cohorts. The result was consistent with that of the long-term trial. In the untreated cohort, the average tumor volume change per day was 84.5 ± 15.7 mm^3 versus 53.4 ± 9.1 mm^3 ($P = 0.108$), 38.1 ± 10.6 mm^3 ($P = 0.033$), and 12.2 ± 14.0 mm^3 ($P = 0.007$), in the IFN-γ-, CCI-779- and combination-treated cohorts, respectively. Although the average tumor volume change per day in the combination-treated cohort was lower than that of the CCI-779-treated cohort, this difference was not statistically significant. This result is consistent with that of the long-term trial where there was no significant difference in average tumor volumes between CCI-779- and combination-treated cohorts at week 2 (Fig. 1a and Table 1).

Effects of CCI-779 and IFN-γ on IFN Regulatory Factor-1 Expression and Cell Death

To understand the mechanism(s) involved in the improved response to combination therapy, we examined molecular markers of apoptosis, cell cycle regulation, and cell proliferation. Immunoblot analysis revealed that tumors from long-term IFN-γ-treated and combination-treated mice expressed higher levels of IFN regulatory factor-1 (IRF-1), in comparison

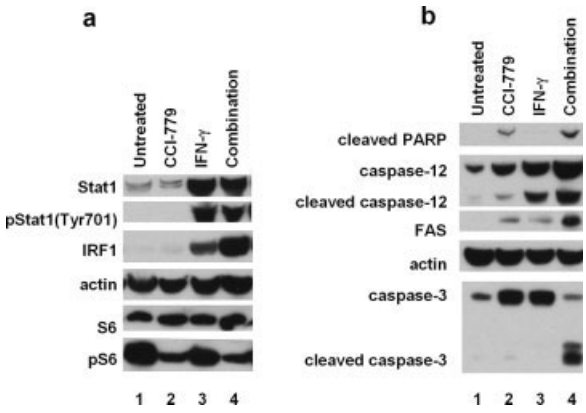

Figure 2. IRF-1 and other markers of cell death in tumors after CCI-779 and/or IFN-γ treatment. Immunoblot analyses of tumors from the long-term treatment trial show the effects of treatment on the levels of proteins involved in apoptosis. (a) Combination-treated tumors express higher IRF-1 levels than do IFN-γ-treated tumors. This result was observed in 9/10 tumors from the combination-treated cohort compared with tumors from the IFN-γ-treated cohort. IRF-1 levels were very low or undetectable in the majority of untreated and CCI-779-treated tumors, as illustrated by the examples in lanes 1 and 2. (b) Combination-treated tumors express higher levels of cleaved PARP, cleaved caspase-12, FAS, and cleaved caspase-3 than do untreated tumors or tumors treated with either CCI-779 or IFN-γ. Three tumors from each cohort were examined for caspase-12, FAS, and cleaved caspase-9 expression, and 3/3 showed the changes described earlier. Elevated levels of cleaved caspase-3 were observed in 7/9 combination-treated tumors, and elevated levels of cleaved PARP were observed in 5/7 combination-treated tumors.

with tumors from untreated or CCI-779-treated mice (Fig. 2a). Interestingly, the increase in IRF-1 levels was consistently more remarkable in combination-treated tumors than in IFN-γ-treated tumors.

IRF-1 is a transcriptional activator whose expression is induced by a number of stimuli, including IFN-γ (Skaar et al., 1998; Taniguchi et al., 2001). More recently, it has been shown that IRF-1 exhibits tumor suppressor activity in breast cancer cells (Kim et al., 2004), and that the antitumor effect of IRF-1 was mediated through caspase activation and induction of apoptosis (Bouker et al., 2005). Consistent with an apoptosis-inducing role for IRF-1, the combination-treated tumors from our long-term trial also express higher levels of other proteins involved in apoptosis: cleaved poly ADP-ribose polymerase (PARP), cleaved caspase-12, FAS, and cleaved caspase-3 (Fig. 2b). This suggests that combination-treated tumors undergo apoptosis at a higher rate than untreated, CCI-779-treated, or IFN-γ-treated tumors, which prompted us to examine apoptosis in greater detail in the short-term-treated tumors.

The expression levels of various caspases in all tumors from the short-term treatment trial were determined by immunoblot analysis. The caspases belong to a family of cysteine aspartate-specific proteases that are involved in apoptosis and inflammation. Caspases are initially produced as inactive zymogens that are activated by proteolysis (Wang et al., 2005). When compared with the levels in untreated tumors, the levels of cleaved (activated) caspase-9 was increased in CCI-779-treated, IFN-γ-treated, and combination-treated tumors by 1.6-, 2.3-, and 1.4-fold, respectively (Figs. 3a and 3c). Cleaved caspase-12 showed a 1.8-fold increase in only the IFN-γ-treated tumors. IFN-γ- and combination-treated tumors from the short-term trial also showed highly elevated levels of IRF-1. However, unlike the observations in the long-term trial, the levels of IRF-1 in the combination-treated tumors were not higher than those in the IFN-γ-treated tumors (Fig. 3b).

The extent of apoptosis in the tumors from the short-term treatment trial was further investigated by a TUNEL assay. Overall, the percentage of apoptotic cells in non-necrotic areas of the tumors was very low, which may be due in part to the short duration of treatment. Nevertheless, CCI-779- and combination-treated tumors had almost twice as many apoptotic cells as untreated or IFN-γ-treated tumors (Table 2). Untreated tumors had a percentage of 1.32 ± 0.25 apoptotic cells versus 2.84 ± 0.32 in CCI-779-treated tumors ($P = 0.004$), and 2.66 ± 0.24 in combination-treated tumors ($P = 0.003$). The similar extent of apoptosis in the CCI-779-treated and combination-treated tumors is consistent with results of the long-term treatment trial, where there was no measurable difference in tumor growth rate between these two cohorts during the first 2 weeks of treatment.

Figure 3. Immunoblot analysis demonstrating that CCI-779 and IFN-γ treatments affect the levels of proteins involved in apoptosis, cell cycle regulation, and cell proliferation in $Tsc2^{-/-}$ tumors. Tumor lysates are from $Tsc2^{-/-}$ tumors from indicated treatment cohorts from the short-term trial. (a) Modest increases in levels of cleaved caspase-9 and cleaved caspase-12 were observed in some tumors after short-term treatment with CCI-779, IFN-γ, or CCI-779 plus IFN-γ. Two exposures for cleaved caspase-9 are shown. (b) Levels of MPP2 (FoxM1), PCNA, and pS6 were reduced by treatment with CCI-779 or CCI-779 plus IFN-γ. Although not shown in this example, levels of MPP2 were also reduced in 3/6 IFN-γ-treated tumors. Levels of Stat1, pStat1 (Ser727), and IRF-1 were increased by treatment with IFN-γ or CCI-779 plus IFN-γ. (c) Densitometry analysis of immunoblots from the short-term treatment trial. Protein expression ratios in all untreated tumors were averaged and normalized to 1.0 (100%). For each indicated protein, the expression ratio for each treated cohort is an average from all tumors within the cohort, and is shown in comparison with the expression ratio of the untreated cohort. The densitometry results for MPP2 differ from the results shown in Fig. 3b because these results were variable and the densitometry analysis measured the average protein expression ratios from six samples per cohort, while the immunoblot shows only one sample.

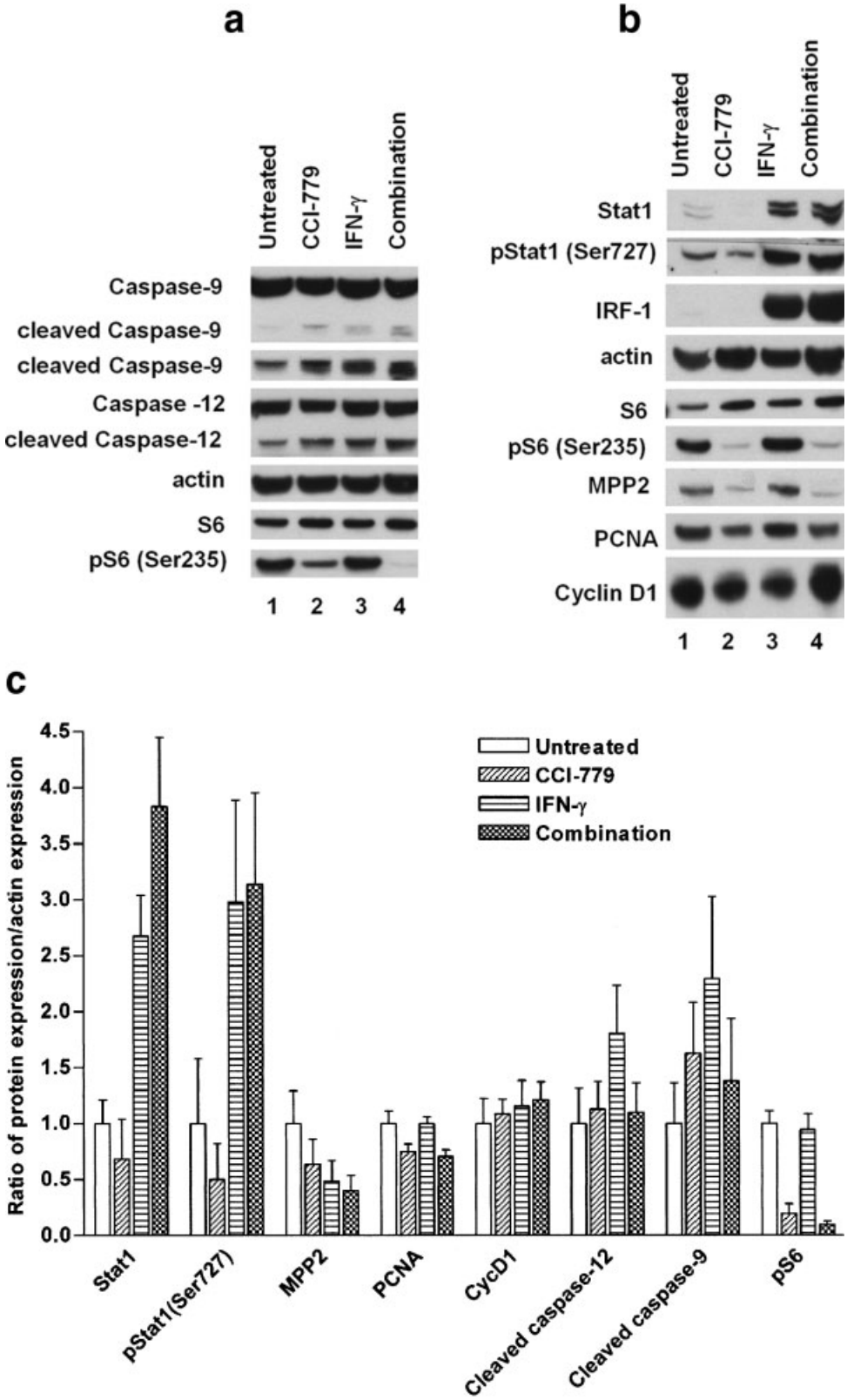
a
Untreated
CCI-779
IFN-γ
Combination
Caspase-9
cleaved Caspase-9
cleaved Caspase-9
Caspase -12
cleaved Caspase-12
actin
S6
pS6 (Ser235)
1 2 3 4
b
Untreated
CCI-779
IFN-γ
Combination
Stat1
pStat1 (Ser727)
IRF-1
actin
S6
pS6 (Ser235)
MPP2
PCNA
Cyclin D1
1 2 3 4
c
Ratio of protein expression/actin expression
4.5
4.0
3.5
3.0
2.5
2.0
1.5
1.0
0.5
0.0
Untreated
CCI-779
IFN-γ
Combination
Stat1
pStat1(Ser727)
MPP2
PCNA
CycD1
Cleaved caspase-12
Cleaved caspase-9
pS6

Figure 3.

TABLE 2. Apoptosis in Tumors from Short-term Treatment Trial

	Untreated	IFN-γ-treated	CCI-779-treated	Combination-treated
% Apoptotic cells	1.3 ± 0.3	1.4 ± 0.2	2.8 ± 0.3	2.7 ± 0.2
P value			0.004*	0.003*
N (mice)	6	6	6	6

*When compared with untreated.

Effects of Treatment on Cell Cycle Regulation and Cell Proliferation

It has been reported that inhibition of mTOR by rapamycin or CCI-779 results in down-regulation of cyclin D1 expression, leading to cell cycle arrest (Hashemolhosseini et al., 1998; Luan et al., 2002; Frost et al., 2004; Dong et al., 2005). To confirm that CCI-779 inhibited the mTOR signal transduction pathway in the $Tsc2^{-/-}$ tumors, the hyperphosphorylation of a well-studied mTOR target, S6 ribosomal protein (S6), was determined by immunoblot analysis. As expected, untreated $Tsc2^{-/-}$ tumors expressed high levels of phospho-S6 (pS6) (Figs. 3a and 3b; lane 1), in contrast to tumors from CCI-779-treated and combination-treated cohorts, which showed diminished pS6 levels (Figs. 3a and 3b; lanes 2 and 4). Similar observations were made in the long-term treatment trial (Fig. 2a).

In the short-term treatment trial, both single agent and combination treatments resulted in decreased levels of MPP2 (FoxM1) (Figs. 3b and 3c). With MPP2 levels in untreated tumors normalized to 100%, the levels in CCI-779-, IFN-γ- and combination-treated tumors were 64, 49, and 40%, respectively. MPP2 is a transcription factor that plays an important role in cell cycle regulation (Laoukili et al., 2005), and elevated levels of MPP2 has been detected in some cancers (Teh et al., 2002; Wonsey and Follettie, 2005). Decreasing the levels of MPP2 may lead to cell cycle arrest and may be one mechanism by which CCI-779 exerts its anti-tumor effect. Interestingly, MPP2 expression was lowest in the combination-treated tumors, suggesting that there may be an additive effect when CCI-779 and IFN-γ are used in combination (Fig. 3c).

CCI-779- and combination-treated tumors also showed a modest but reproducible decrease in the levels of proliferating cell nuclear antigen (PCNA), a protein associated with DNA synthesis (Figs. 3b and 3c). PCNA levels in CCI-779- and combination-treated tumors were 75% and 71%, respectively, when compared with that in untreated tumors (normalized to 100%). This suggests that cell proliferation is negatively affected by CCI-779 and combination treatments. We were unable to detect any significant difference in cyclin D1 levels between untreated and CCI-779-treated tumors.

Immunoblot analyses of tumors from the long-term treatment trial was also carried out to determine the levels of the cell cycle and cell proliferation proteins mentioned earlier. However, no significant differences were observed between treated and untreated tumors (data not shown). This was not surprising, since all tumors had resumed progressive growth by the time of analysis.

Exogenous IFN-γ Activates the JAK-STAT Signal Transduction Pathway in $Tsc2^{-/-}$ Tumors

Since IFN-γ signals primarily through the JAK-STAT signal transduction pathway, we sought to verify that exogenous IFN-γ also activates this pathway in the $Tsc2^{-/-}$ tumors. Immunoblot analyses of tumor lysates from both the long-term and short-term treatment trials confirmed that the JAK-STAT pathway was activated by IFN-γ. Tumors from the IFN-γ-treated and combination-treated cohorts showed elevated levels of Stat1, phospho-Stat1 (pStat1), and IRF-1 (Figs. 2a and 3b). The marked induction of Stat1 by IFN-γ is particularly interesting because of the emerging evidence that Stat1 may act as a tumor suppressor by inhibiting cell growth and promoting apoptosis (Bromberg, 2001; Stephanou and Latchman, 2003). Therefore, Stat1 induction may be one mechanism by which IFN-γ inhibits tumor growth in this mouse model of TSC.

Molecular Analysis of $Tsc2^{-/-}$ Cultured Cells Treated with CCI-779 and IFN-γ

Since there was some variability in tumors within each cohort in terms of clinical response to treatment and treatment-induced biochemical changes, we also tested the effects of CCI-779 and IFN-γ on cultured cells. $Tsc2^{-/-}$ cells were treated with CCI-779, IFN-γ, or both agents for 3, 24, 48, and 72 hr, and immunoblot analysis was carried out to determine the effects of treatment(s) on the levels of proteins involved in cell cycle regulation, cell proliferation, and apoptosis.

The inhibitory effect of CCI-779 on mTOR was verified by the marked decrease in pS6 levels

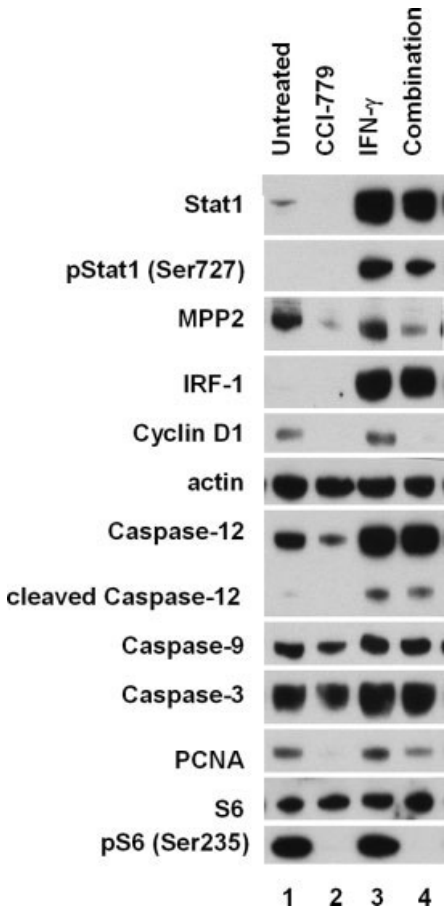

Figure 4. Markers of apoptosis, cell cycle regulation, cell proliferation, mTOR activation, and JAK-STAT pathway activation in cultured $Tsc2^{-/-}$ cells. Cell lysates are from $Tsc2^{-/-}$ cells treated for 24 hr with CCI-779 (20 nM), IFN-γ (10 ng/ml), or the combination of these two drugs (at the doses indicated). Increased levels of markers of apoptosis (caspase-12, cleaved caspase-12, and IRF-1) and decreased levels of markers of cell proliferation (MPP2, cyclin D1, and PCNA) were observed in cultured $Tsc2^{-/-}$ cells treated with CCI-779 plus IFN-γ. Increased caspase-12, cleaved caspase-12, and IRF-1 were observed with IFN-γ treatment. Decreased MPP2, cyclin D1 and PCNA were observed with CCI-779 treatment. Also shown are decreased pS6 expression in cells treated with CCI-779 or CCI-779 plus IFN-γ, and elevated Stat1, pStat1, and IRF-1 in cells treated with IFN-γ or CCI-779 plus IFN-γ. Similar observations were made in cells treated for 3, 48, and 72 hr.

(Fig. 4; lanes 2 and 4). Activation of the JAK-STAT signaling pathway by IFN-γ was verified by an increase in protein levels of Stat1, pStat1, and IRF-1 (lanes 3 and 4). Cultured $Tsc2^{-/-}$ cells treated with IFN-γ or CCI-779 plus IFN-γ showed a marked increase in the levels of both pro and cleaved caspase-12 (lanes 3 and 4). However, levels of pro and cleaved caspase-9 and caspase-3 were not affected by either CCI-779 or IFN-γ. CCI-779 down-regulated MPP2 and PCNA levels, which is consistent with our observations in the $Tsc2^{-/-}$ tumors. In addition, CCI-779 treatment also resulted in decreased levels of cyclin D1 (lanes 2 and 4).

DISCUSSION

We have shown that combined CCI-779 and IFN-γ treatment is more effective than CCI-779 treatment in reducing tumor growth and improving survival in a nude mouse model of TSC. The advantage of combination treatment only becomes apparent during weeks 3–6 of treatment in the long-term treatment trial in which tumor-bearing mice were treated for up to 6 weeks. Interestingly, we observed a marked increase in IRF-1 tumor suppressor levels in the combination-treated tumors at week 6 (long-term trial), but not at week 1 (short-term trial) of treatment. This suggests that increased levels of IRF-1 induced by IFN-γ after prolonged treatment may be an important mediator of the enhanced antitumor effect of combination treatment.

Treatment with IFN-γ as a single agent only had minimal effect on tumor growth, in contrast to our observations in a previous trial where IFN-γ significantly reduced the severity of TSC-related disease (Lee et al., 2005). This is likely due to the difference between the two trials in the timing of treatment. In the previous trial, treatment was initiated at a much lower tumor volume (6.7 ± 3.2 mm^3), in contrast to the current trial in which the average tumor volume at the start of treatment was 499.7 ± 24.7 mm^3. These results suggest that IFN-γ is more effective as an antitumor agent when used earlier (when tumors are smaller), and warrant further investigation.

Molecular analyses focusing on mTOR signaling, IFN-γ signaling, apoptosis, and cell cycle regulation demonstrate that additive or synergistic effects may explain the improved response in the combination-treated tumors. In addition to activation of the IFN-γ signaling pathway, as demonstrated by elevated levels of IFN-γ inducible proteins (Stat1, pStat1 and IRF-1), combination-treated tumors also had reduced mTOR activity, and other changes consistent with decreased cell proliferation and increased apoptosis. Elevated levels of IRF-1, cleaved caspase-12, cleaved caspase-3, cleaved PARP, and FAS were initially observed in combination-treated tumors in the long-term trial, which prompted a further investigation of additional markers of apoptosis. In a short-term trial, the extent of apoptosis in combination-treated and CCI-779-treated tumors was higher than in untreated or IFN-γ-treated tumors. This indicates that CCI-779 induces apoptosis, which is consistent with the higher levels of cleaved caspase-9 found in CCI-779-treated tumors. Others

have also reported that rapamycin or CCI-779 may exert an antitumor effect by inducing apoptosis (El-Hashemite et al., 2004; Frost et al., 2004; Avellino et al., 2005; Kenerson et al., 2005; Schachner et al., 2005). The fact that the IFN-γ-treated tumors did not exhibit more apoptosis than untreated tumors is puzzling, given our observations of elevated cleaved caspases in these tumors. A possible explanation is that IFN-γ-induced apoptosis occurs later than CCI-779-induced apoptosis; consequently, apoptosis was not detected after only 2–5 treatments. Additionally, the IFN-γ-treated cohort received fewer treatments on average than did the CCI-779-treated or combination-treated cohorts. Similar to the biochemical characteristics of the CCI-779-treated tumors, the combination-treated tumors had increased cleaved caspase-9, indicating increased apoptosis, as well as reduced levels of PCNA and MPP2, indicating decreased cell proliferation.

Because of tumor tissue heterogeneity and the subtlety of some of our results, we also investigated mTOR signaling, IFN-γ signaling, apoptosis, and cell proliferation in cultured $Tsc2^{-/-}$ cells treated with combined IFN-γ plus CCI-779. The cell culture experiments confirmed our findings in the $Tsc2^{-/-}$ tumor tissue as cultured $Tsc2^{-/-}$ cells treated with both IFN-γ and CCI-779 also exhibited molecular changes consistent with a decrease in cell proliferation and an increase in apoptosis: decreased MPP2, cyclin D1 and PCNA, and increased Stat1, IRF-1, pro-caspase-12, and cleaved caspase-12.

Taken together, the molecular analyses from both treatment trials and cell culture experiments indicate that treatment with CCI-779 plus IFN-γ induces the expression of potential tumor suppressors (IRF-1 and Stat1) and apoptosis markers (cleaved PARP, FAS, and cleaved caspases), and decreases the levels of cell cycle regulators (MPP2 and cyclin D1) and a cell proliferation marker (PCNA). These observations strongly suggest that the increased efficacy of combination treatment is due to the combined effects of inhibition of cell proliferation and induction of cell death.

Tumor growth kinetics in the CCI-779- and combination-treated tumors from the long-term trial demonstrate that tumor regression occurs initially but ultimately these tumors grow again. It has been observed that cells and tumors can develop resistance to rapamycin (Hosoi et al., 1998; Huang and Houghton, 2001; Dilling et al., 2002; Chen et al., 2003); so, this resumption of progressive growth could be due to the tumors developing resistance to CCI-779. During the first 2 weeks of treatment, the majority of tumors in both combination-treated and CCI-779-treated cohorts regressed, resulting in average tumor volume decreases in both of these treatment cohorts. Beyond 2 weeks of treatment, however, the tumors resumed progressive growth, but the tumors in the combination-treated cohort grew at a significantly slower rate than those in the CCI-779-treated cohort. In our experiment, it appears that the tumors in the CCI-779-treated cohort were still responding partially to CCI-779 after week 2, because their average growth rate (110.2 ± 15.7 mm^3/day) was still significantly lower than the average growth rate of tumors in the untreated cohort (222.1 ± 26.35 mm^3/day). We observed low levels of pS6 but no reduction of PCNA or other cell cycle regulators in CCI-779- and combination-treated tumors from the long-term trial, which suggests that resistance occurs despite evidence for effective inhibition of mTOR activity.

In conclusion, we have shown in a nude mouse model of TSC that combined CCI-779 plus IFN-γ treatment is more effective than treatment with CCI-779 in reducing tumor growth and improving survival. Our results indicate that combination treatment exerts its antitumor effect by inhibiting cell proliferation and inducing cell death. Our finding is relevant, given that drug resistance is a potential problem in the efforts to develop rapamycin and its analogs as targeted therapy for TSC. A study examining the antitumor effects of rapamycin in a rat model of TSC provided some evidence for rapamycin resistance in a small percentage of lesions after prolonged therapy (Kenerson et al., 2005). Even though the improved efficacy of combined CCI-779 and IFN-γ over CCI-779 alone was not very high, our results underscore the importance of developing rapamycin in combination with other agents as treatment therapy for TSC. Our results demonstrate that manipulating multiple cellular pathways simultaneously (i.e., inducing apoptosis and inhibiting cell growth) is a useful strategy for treating TSC-related tumors, and provides preclinical evidence to justify investigating combination therapy in future clinical trials for patients with TSC and related disorders.

ACKNOWLEDGMENTS

The authors thank Jay Gibbons at Wyeth-Ayerst Pharmaceuticals for providing CCI-779 for this work, and Michael Messina and Aubrey Rauktys for technical assistance.

REFERENCES

Avellino R, Romano S, Parasole R, Bisogni R, Lamberti A, Poggi V, Venuta S, Romano MF. 2005. Rapamycin stimulates apoptosis of childhood acute lymphoblastic leukemia cells. Blood 106:1400–1406.

Bissler J, Franz D, McCormack FX, Chuck G, Leonard J, Young L, Elwing J. 2004. Rapamycin therapy of AMLs in patients with TSC and sporadic LAM. Data presented at TSC Conference, Cambridge, UK, Sept. 2004.

Bouker KB, Skaar TC, Riggins RB, Harburger DS, Fernandez DR, Zwart A, Wang A, Clarke R. 2005. Interferon regulatory factor-1 (IRF-1) exhibits tumor suppressor activities in breast cancer associated with caspase activation and induction of apoptosis. Carcinogenesis 26:1527–1535.

Bromberg JF. 2001. Activation of STAT proteins and growth control. Bioessays 23:161–169.

Cheadle JP, Reeve MP, Sampson JR, Kwiatkowski DJ. 2000. Molecular genetic advances in tuberous sclerosis. Hum Genet 107:97–114.

Chen Y, Zheng Y, Foster DA. 2003. Phospholipase D confers rapamycin resistance in human breast cancer cells. Oncogene 22:3937–3942.

Dabora SL, Jozwiak S, Franz DN, Roberts PS, Nieto A, Chung J, Choy YS, Reeve MP, Thiele E, Egelhoff JC, Kasprzyk-Obara J, Domanska-Pakiela D, Kwiatkowski DJ. 2001. Mutational analysis in a cohort of 224 tuberous sclerosis patients indicates increased severity of TSC2, compared with TSC1, disease in multiple organs. Am J Hum Genet 68:64–80.

Dabora SL, Roberts P, Nieto A, Perez R, Jozwiak S, Franz D, Bissler J, Thiele EA, Sims K, Kwiatkowski DJ. 2002. Association between a high-expressing interferon-γ allele and a lower frequency of kidney angiomyolipomas in TSC2 patients. Am J Hum Genet 71:750–758.

Dilling MB, Germain GS, Dudkin L, Jayaraman AL, Zhang X, Harwood FC, Houghton PJ. 2002. 4E-binding proteins, the suppressors of eukaryotic initiation factor 4E, are down-regulated in cells with acquired or intrinsic resistance to rapamycin. J Biol Chem 277:13907–13917.

Dong J, Peng J, Zhang H, Mondesire WH, Jian W, Mills GB, Hung MC, Meric-Bernstam F. 2005. Role of glycogen synthase kinase 3β in rapamycin-mediated cell cycle regulation and chemosensitivity. Cancer Res 65:1961–1972.

El-Hashemite N, Zhang H, Walker V, Hoffmeister KM, Kwiatkowski DJ. 2004. Perturbed IFN-γ-Jak-signal transducers and activators of transcription signaling in tuberous sclerosis mouse models: Synergistic effects of rapamycin-IFN-γ treatment. Cancer Res 64:3436–3443.

Findlay GM, Harrington LS, Lamb RF. 2005. TSC1-2 tumour suppressor and regulation of mTOR signalling: Linking cell growth and proliferation? Curr Opin Genet Dev 15:69–76.

Franz DN, Brody A, Meyer C, Leonard J, Chuck G, Dabora S, Sethuraman G, Colby TV, Kwiatkowski DJ, McCormack FX. 2001. Mutational and radiographic analysis of pulmonary disease consistent with lymphangioleiomyomatosis and micronodular pneumocyte hyperplasia in women with tuberous sclerosis. Am J Respir Crit Care Med 164:661–668.

Frost P, Moatamed F, Hoang B, Shi Y, Gera J, Yan H, Gibbons J, Lichtenstein A. 2004. In vivo antitumor effects of the mTOR inhibitor CCI-779 against human multiple myeloma cells in a xenograft model. Blood 104:4181–4187.

Gao X, Zhang Y, Arrazola P, Hino O, Kobayashi T, Yeung RS, Ru B, Pan D. 2002. Tsc tumour suppressor proteins antagonize amino-acid No. 150; TOR signalling. Nat Cell Biol 4:699–704.

Garber K. 2001. Rapamycin's resurrection: A new way to target the cancer cell cycle. J Natl Cancer Inst 93:1517–1519.

Gomez MR. 1995. History of the tuberous sclerosis complex. Brain Dev 17 Suppl:55–57.

Hashemolhosseini S, Nagamine Y, Morley SJ, Desrivieres S, Mercep L, Ferrari S. 1998. Rapamycin inhibition of the G1 to S transition is mediated by effects on cyclin D1 mRNA and protein stability. J Biol Chem 273:14424–14429.

Hidalgo M, Rowinsky EK. 2000. The rapamycin-sensitive signal transduction pathway as a target for cancer therapy. Oncogene 19:6680–6686.

Hino O, Kobayashi T, Mitani H. 2002. Prevention of hereditary carcinogenesis. Proc Jpn Acad 78:30–32.

Hosoi H, Dilling MB, Liu LN, Danks MK, Shikata T, Sekulic A, Abraham RT, Lawrence JC, Jr., Houghton PJ. 1998. Studies on the mechanism of resistance to rapamycin in human cancer cells. Mol Pharmacol 54:815–824.

Huang S, Houghton PJ. 2001. Resistance to rapamycin: A novel anticancer drug. Cancer Metastisis Rev 20:69–78.

Inoki K, Corradetti MN, Guan KL. 2005. Dysregulation of the TSC-mTOR pathway in human disease. Nat Genet 37:19–24.

Kenerson H, Dundon TA, Yeung RS. 2005. Effects of rapamycin in the Eker rat model of tuberous sclerosis complex. Pediatr Res 57:67–75.

Kenerson HL, Aicher LD, True LD, Yeung RS. 2002. Activated mammalian target of rapamycin pathway in the pathogenesis of tuberous sclerosis complex renal tumors. Cancer Res 62:5645–5650.

Kim PK, Armstrong M, Liu Y, Yan P, Bucher B, Zuckerbraun BS, Gambotto A, Billiar TR, Yim JH. 2004. IRF-1 expression induces apoptosis and inhibits tumor growth in mouse mammary cancer cells in vitro and in vivo. Oncogene 23:1125–1135.

Kwiatkowski DJ, Short MP. 1994. Tuberous sclerosis. Arch Dermatol 130:348–354.

Kwiatkowski DJ, Zhang H, Bandura JL, Heiberger KM, Glogauer M, El-Hashemite N, Onda H. 2002. A mouse model of TSC1 reveals sex-dependent lethality from liver hemangiomas, and up-regulation of p70S6 kinase activity in Tsc1 null cells. Hum Mol Genet 11:525–534.

Laoukili J, Kooistra MR, Bras A, Kauw J, Kerkhoven RM, Morrison A, Clevers H, Medema RH. 2005. FoxM1 is required for execution of the mitotic programme and chromosome stability. Nat Cell Biol 7:126–136.

Lee L, Sudentas P, Donohue B, Asrican K, Worku A, Walker V, Sun Y, Schmidt K, Albert MS, El-Hashemite N, Lader AS, Onda H, Zhang H, Kwiatkowski DJ, Dabora SL. 2005. Efficacy of a rapamycin analog (CCI-779) and IFN-γ in tuberous sclerosis mouse models. Genes Chromosomes Cancer 42:213–227.

Luan FL, Hojo M, Maluccio M, Yamaji K, Suthanthiran M. 2002. Rapamycin blocks tumor progression: Unlinking immunosuppression from antitumor efficacy. Transplantation 73:1565–1572.

Meraz MA, White JM, Sheehan KC, Bach EA, Rodig SJ, Dighe AS, Kaplan DH, Riley JK, Greenlund AC, Campbell D, Carver-Moore K, DuBois RN, Clark R, Aguet M, Schreiber RD. 1996. Targeted disruption of the *Stat*1 gene in mice reveals unexpected physiologic specificity in the JAK-STAT signaling pathway. Cell 84:431–442.

Mills GB, Lu Y, Kohn EC. 2001. Linking molecular therapeutics to molecular diagnostics: Inhibition of the FRAP/RAFT/TOR component of the PI3K pathway preferentially blocks PTEN mutant cells in vitro and in vivo. Proc Natl Acad Sci USA 98:10031–10033.

Neshat MS, Mellinghoff IK, Tran C, Stiles B, Thomas G, Petersen R, Frost P, Gibbons JJ, Wu H, Sawyers CL. 2001. Enhanced sensitivity of PTEN-deficient tumors to inhibition of FRAP/mTOR. Proc Natl Acad Sci USA 98:10314–10319.

Online Mendelian Inheritance in Man O. 2003a. MIM number 606690. Baltimore, MD: Johns Hopkins University.

Online Mendelian Inheritance in Man O. 2003b. MIM numbers 605284 and 191092. Baltimore, MD: Johns Hopkins University.

Podsypanina K, Lee RT, Politis C, Hennessy I, Crane A, Puc J, Neshat M, Wang H, Yang L, Gibbons J, Frost P, Dreisbach V, Blenis J, Gaciong Z, Fisher P, Sawyers C, Hedrick-Ellenson L, Parsons R. 2001. An inhibitor of mTOR reduces neoplasia and normalizes p70/S6 kinase activity in Pten$^{+/-}$ mice. Proc Natl Acad Sci USA 98:10320–10325.

Potter CJ, Huang H, Xu T. 2001. Drosophila Tsc1 functions with Tsc2 to antagonize insulin signaling in regulating cell growth, cell proliferation, and organ size. Cell 105:357–368.

Schachner T, Oberhuber A, Zou Y, Tzankov A, Ott H, Laufer G, Bonatti J. 2005. Rapamycin treatment is associated with an increased apoptosis rate in experimental vein grafts. Eur J Cardiothorac Surg 27:302–306.

Schroder K, Hertzog PJ, Ravasi T, Hume DA. 2004. Interferon-γ: An overview of signals, mechanisms and functions. J Leukoc Biol 75:163–189.

Skaar TC, Prasad SC, Sharareh S, Lippman ME, Brunner N, Clarke R. 1998. Two-dimensional gel electrophoresis analyses identify nucleophosmin as an estrogen regulated protein associated with acquired estrogen-independence in human breast cancer cells. J Steroid Biochem Mol Biol 67:391–402.

Stephanou A, Latchman DS. 2003. STAT-1: A novel regulator of apoptosis. Int J Exp Pathol 84:239–244.

Taniguchi T, Ogasawara K, Takaoka A, Tanaka N. 2001. IRF family of transcription factors as regulators of host defense. Annu Rev Immunol 19:623–655.

Teh MT, Wong ST, Neill GW, Ghali LR, Philpott MP, Quinn AG. 2002. FOXM1 is a downstream target of Gli1 in basal cell carcinomas. Cancer Res 62:4773–4780.

Torrance CJ, Agrawal V, Vogelstein B, Kinzler KW. 2001. Use of isogenic human cancer cells for high-throughput screening and drug discovery. Nat Biotechnol 19:940–945.

Vignot S, Faivre S, Aguirre D, Raymond E. 2005. mTOR-targeted therapy of cancer with rapamycin derivatives. Ann Oncol 16:525–537.

Wang ZB, Liu YQ, Cui YF. 2005. Pathways to caspase activation. Cell Biol Int 29:489–496.

Wienecke R, Fackler I, Akdeli N, Linsenmaier U, Vogeser M, Mayer K, Licht T, Kretzler M. 2004.Effective treatment of TSC with rapamycin. Data presented at TSC Conference, Cambridge, UK, Sept. 2004.

Wonsey DR, Follettie MT. 2005. Loss of the forkhead transcription factor FoxM1 causes centrosome amplification and mitotic catastrophe. Cancer Res 65:5181–5189.

Yu K, Toral-Barza L, Discafani C, Zhang WG, Skotnicki J, Frost P, Gibbons JJ. 2001. mTOR, a novel target in breast cancer: The effect of CCI-779, an mTOR inhibitor, in preclinical models of breast cancer. Endocr Relat Cancer 8:249–258.